A new growth approach to fabricate CuMo alloy nanowires

A Thesis Presented

By

ÈRIC NAVARRETE GATELL

to

The Department of Chemical Engineering

In partial fulfillment of the requirements

For the degree of

Master in Nanoscience, Materials and Processes:

Chemical technology at the frontier.

In the field of

Chemical Engineering

Universitat Rovira i Virgili

Tarragona, Spain

Northeastern University

Boston, Massachusetts

July 29, 2016

1. Introduction

Molybdenum is a metal commonly used in industrial processes due to its good thermal and electrical conductivity, low thermal expansion, high melting point, low vapor pressure, high temperature resistance, and high wear resistance.[17] When this metal is used as an alloying material it has been found to boost both mechanical properties and corrosion resistance of such alloys.[4] Furthermore, molybdenum as well as tungsten has the property of catalyzing the formation of hydrogen from aqueous solvents which is typically found on noble metals such as platinum.[1,3] Therefore, molybdenum has recently become a promising material to use in hydrogen fuel cells to replace expensive noble metals, resulting in a more economically competitive source of renewal energy.

Even though that there are several methodologies to obtain molybdenum alloys such as from melt or powder composites, electrodeposition is a less expensive technique, and has the potential to fill small recessed structures to create nanostructured materials. A challenge of the electrodeposition process for the deposition of molybdenum alloys is that it is difficult to obtain a high molybdenum concentration into alloys from aqueous solution, and the deposition mechanism is not well understood. Due to its unique characteristic, molybdenum, as well as tungsten, can't be electrodeposited alone, as a single element, from aqueous solution, but can be reduced along with an additional inducing element, such as nickel.[12] This behavior, referred to as induced co-deposition, was first reported in the earlier 1930's by Brenner.[5] Brenner was the author of several works related with molybdenum and tungsten alloy electrodeposition as well as the one who coined the co-deposition behavior term.[7] The reduction of molybdenum or tungsten can occur with metals from the iron group: iron, nickel and cobalt, as well as some recent reports with Cu and Ag.[14] Despite several years of research, there is still not a consensus about the mechanism involved in co-deposition, although several authors have proposed different mechanism[8,9,10,11] but none of them completely explain the process.

Despite the fact that the mechanism involved is not fully known, the ability of the iron group metals to co-deposit this metal leads to higher concentrations of molybdenum, while using other metals leads to poor concentration of molybdenum on such alloys. The challenge present in this field is obtaining different metal-molybdenum alloys with higher concentrations of molybdenum by electrodeposition; as it has been mentioned above molybdenum enhances different properties of interest depending on

the specific requirements, such as low thermal expansion coefficient which helps on removing heat once the current is flowing through them on semiconductor devices.[6] Furthermore, reviewing its catalytic ability to produce hydrogen has a huge interest, when such alloys are being grown, this reaction also takes place which means that the surface where the electrodeposition is being performed can suffer from the formation of hydrogen bubbles; if they are incorporated into the alloy structure they may lead to weak points potentially leading to breakage. When those alloys have macroscopic dimensions like thick films the formation of those hydrogen bubbles don't represent a drawback. But once the dimensions are decreased and new nanostructured composites are required, such as nanowires the hydrogen formation becomes a challenging drawback that should be avoided. To minimize the effect of hydrogen formation it has been probed that using surfactants, such as sodium lauryl sulfate, in low concentration could lead to the decrease of the size bubbles as well as enable their removal. However, higher concentrations of those types of additives has been found to inhibit the deposition rate and also once incorporated into the structure they can cause distortion and weak points resulting in a stress for the material.[15]

The main aim of this thesis is to present a novel way to electrodeposit copper-molybdenum nanowires in a two steps methodology, that has never been reported before where Fe-Mo, Ni-Mo and Fe-Ni-Mo nanowires are grown and then used to generate, in a novel way, Cu-Ni-Fe-Mo, Cu-Fe-Mo or Cu-Mo, to be used as heat skin power integrated circuits in hybrid vehicles and mobile telephone cell transmitters as high performance advanced material, and as a catalyst for water splitting reaction.[2,16]

As it is well known, when metallic iron is placed in an aqueous solution rich in an electrolyte with a dissolved copper salt a displacement reaction between the solid metal and metal ions occurs, leading to a substitution of the metallic iron which will be incorporated as iron (II) in the aqueous solution and substituted by the metallic copper as it is reduced from copper (II) to solid copper. Therefore, once iron-molybdenum nanowires are obtained they can be treated under the proper conditions with a solution of copper (II) to achieve the removal of a part or all of iron and nickel, and the subsequently substitution by copper leading to rich molybdenum-copper nanowires.

2. Copper displacement approach

The copper displacement approach is based on the thermodynamic activity series of metals. In this work, iron and nickel are used as a more noble element and its reaction with copper ions has a larger potential that drives the anodic reaction of less noble species, compensated by the cathodic reduction of copper ions. The Gibbs free energy of this reaction at standard conditions is given below for the displacement reaction of Cu(II) ions with Fe and Ni.

- $Fe_{(s)} + CuSO_4 \rightarrow Cu_{(s)} + FeSO_{4(aq)}$
    - Oxidation: $Fe_{(s)} \rightarrow Fe^{2+} + 2e^-$
    - Reduction: $Cu^{2+} + 2e^- \rightarrow Cu_{(s)}$
        - **ΔG = - 144,75 kJ**
- $Ni_{(s)} + CuSO_4 \rightarrow Cu_{(s)} + NiSO_{4(aq)}$
    - Oxidation: $Ni_{(s)} \rightarrow Ni^{2+} + 2e^-$
    - Reduction: $Cu^{2+} + 2e^- \rightarrow Cu_{(s)}$
        - **ΔG = - 15,44 kJ**

As presented, both reactions are thermodynamically spontaneous, but as can be inferred from the free energy Gibb's values the nickel reaction is about 10 times lower in energy than the iron reaction. These values do not determine directly the reaction rate, as kinetic and transport limitations often dominate, and thus are presented to show that the reaction is indeed spontaneous.

For the present work, conditions to deposit Mo-alloy nanowires are first presented. The nanowires were deposited from a boric acid-citrate electrolyte. These nanowires were then treated in an acid, copper sulfate solution to facilitate the displacement reaction and thus replace Fe or Ni with Cu, leading to novel Cu-Mo-alloys. Both the precursor nanowires and the Cu-Mo-alloy nanowires are novel.

3. Experimental

3.1. Electrodeposition

The electrodeposition was performed on a standard cell with three electrodes: the working, the counter and the reference electrode. Fig. 1 shows a schematic illustration

of electrolytic cell. *Hummer ™ 6.2 ANATECH USA* sputtering model was used to coat a polycarbonate membrane with a 200 nm thick gold layer under the conditions of 15 mA, 5 minutes and 70 mTorr argon pressure atmosphere. The gold layer has two main purposes, to act as a conductive layer to enable the contact between the membrane and the cathode, and to block one end of the pores. The membrane was placed on the cathode, once attached, the template surface exposed range from 1.98 cm^2 up to 2.37 cm^2 and the total current used was in function of the area exposed.

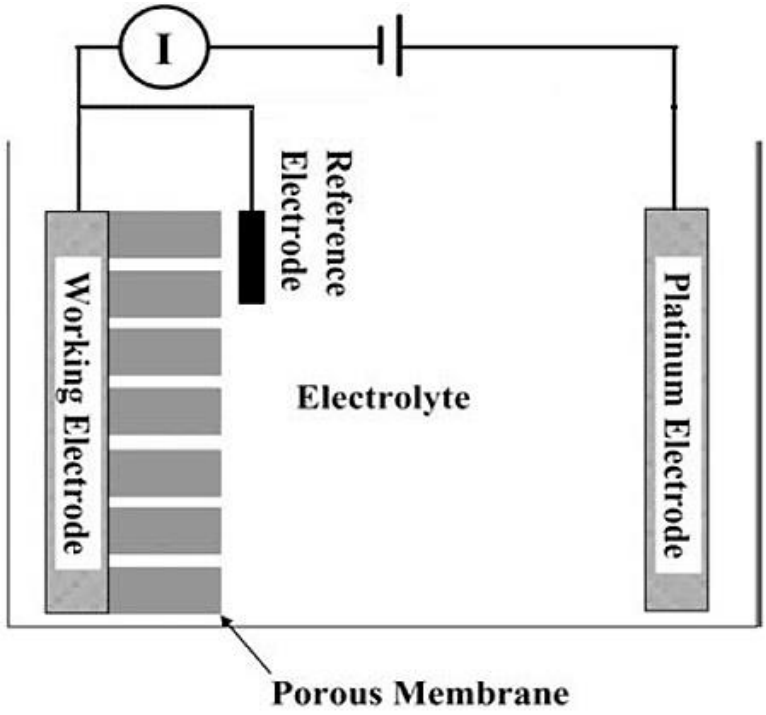


Figure 1. Schematic representation of an electrolytic cell where the nanowires growth is done.

Different tests were done to determine an appropriate electrodeposition mode to achieve robust, continuous nanowires; the electrodeposition with the best results was performed under pulsed current in the three alloys. The pulsed electrodeposition consists of applying a voltage to the working electrode for a set time, called the *on-time*, and applying a zero current, or the open circuit potential, for a set time, called the *off-time*. The main purpose of these cycles is to enable the bubbles of hydrogen formed during the *on-time* to be removed from the system, preventing the blockage of the pores.

To grow nanowires, it is noted that the length is function of time; a first growth to the top was performed to establish the total growth time. Once set, the total growth time for the applied current, the length, can be controlled as function of time.

4. Results

4.1. Fe-Mo nanowires

An attempt to electrodeposit iron/molybdenum nanowires directly onto a polycarbonate membrane template, was made with a pore diameter that has a variable size, smallest at the bottom and reported to be 0.05 microns by the manufacturer. The length of the pores are 6 microns from bottom to top and a porosity of 10 %. The electrodeposition was carried out from an electrolyte containing: 0.1 M ferrous sulfate, 0.02 M sodium molybdate (VI), 0.4 M trisodium citrate, 0.001 M sodium lauryl sulfate, 0.5 M boric acid, 0.002 M saccharine, 0.75 M boric acid at an adjusted pH of 1.5, 4, 8 with H_2SO_4 or NaOH and at a temperature of 40 ^oC and a constant stirring of 300 rpm.

Before deposition, a potentiodynamic scan from 0 V to -2 V vs SCE at a scan rate of 5 mV/s is performed to find the best potential range to set up the growth. Fig. 2 shows a plot using an electrolyte with different amounts of added surfactant. In all cases there is a peak at -1 V vs SCE, which give information about a reaction taking place, and thus, the deposition of the metals therefore is expected to start at potentials more negative than -1 V vs SCE. Furthermore, the plot shows a smooth curve up to -1 V vs SCE, after the peak the curve is rough which is typically found when hydrogen is formed and its bubbles are being generated and simultaneously leaving the surface.

As expected, a great hydrogen catalytic activity occurs from the composition of these nanowire alloys. Therefor the addition of a surfactant, sodium lauryl sulfate (SLS), is strongly recommended, with the aim of decreasing the size of the hydrogen bubbles and enable its removal. The addition of the additive in the electrolytic solution can enhance the deposition of metal, but also can inhibit the reaction, consequently the amount of surfactant should be keep at the lowest concentration, enough to perform its role without affecting the reaction. Three tests with different concentrations of SLS have been done; the concentration range was 0 mM, 1 mM and 8 mM which is the critical micelle concentration (CMC) for this compound. Fig. 2 shows the result with each concentration, as it can be interfered from the plot the best concentration is 1 mM which presents a well-defined peak and a smooth curve.

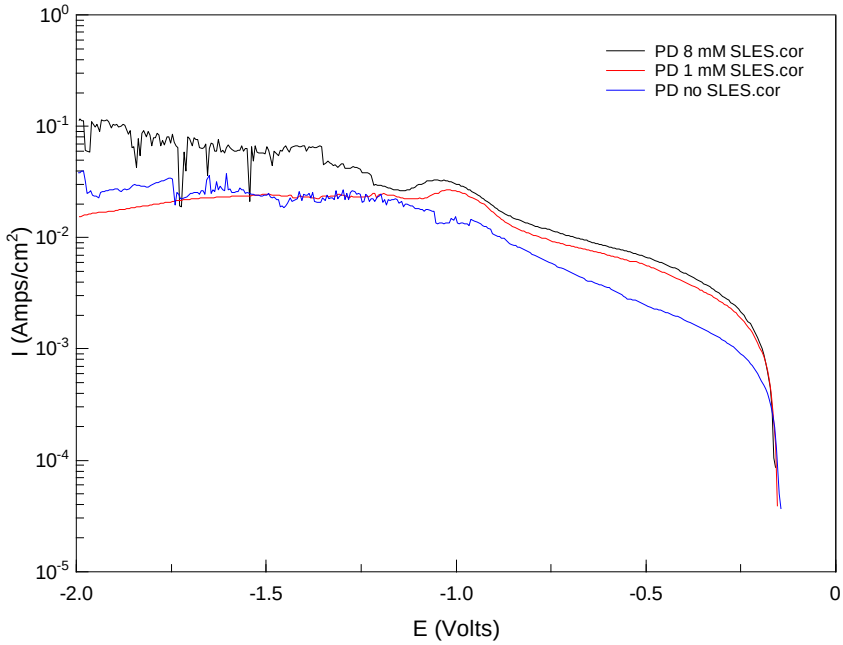


Figure 2. Comparison of the three potentiodynamic studies for all three concentrations of surfactant studied using a SCE electrode as reference.

The nanowires were attempted to be deposited at pH 1.5, 4 and 8 using the pulsed potential method with an "on" and "off" time of 2 seconds each; this avoids the formation of hydrogen bubbles preventing the distortion of the nanowires structure, and the selected potentials were -0.5 V to -1.5 V vs SCE. The potential selected for the "off" time is -0.5 V vs SCE because superior potentials can lead to an undesired positive intensity, therefore this potential keeps the intensity at values close to 0. To ensure that the deposition takes place after the peak located at -1 V vs SCE. The plot obtained for pH 4 is shown in the Fig. 3, where can be interfered that the intensity of the system grows in a conic form Fig. 4, when this behavior occurs at any experiment nanowires were obtained, this behavior occurred during the growth for all three pHs. The total growth time in all experiments were 3500 seconds.

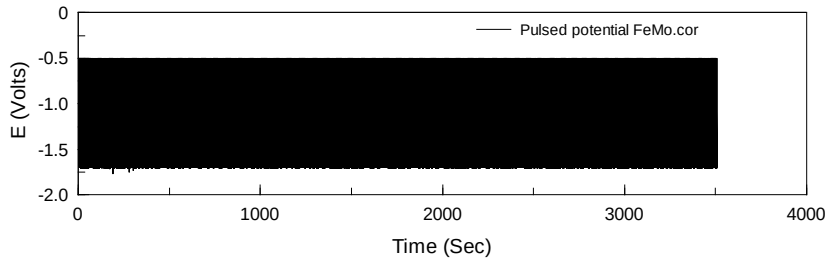


Figure 3. Pulsed potential plot for Fe-Mo nanowires obtained during their growth.

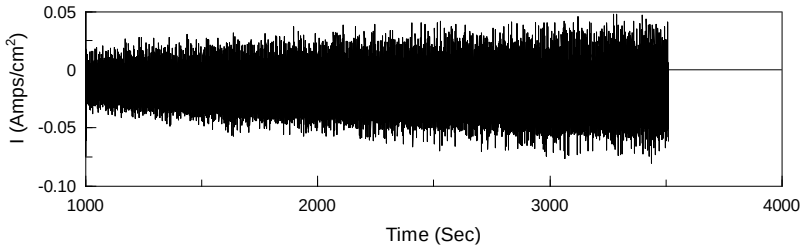


Figure 4. Intensity variation plot in conical growing form.

As stated before for this set of experiments the nanowires were unable to be grown due to the high amount of hydrogen produced during the experiment. Therefore, they can't be reported.

4.2. Ni-Mo nanowires

Nickel/molybdenum nanowires were attempted to be electrodeposit with the same type of polycarbonate membrane template. The electrodeposition was carried out from a similar electrolyte as in the Fe-Mo attempt, except that the Fe was replaced by Ni ions, containing: 0.1 M nickel sulfate, 0.01 M sodium molybdate (VI), 0.4 M trisodium citrate, 0.001 M sodium lauryl sulfate, 0.5 M boric acid, 0.002 M saccharine, 1 M boric acid at an adjusted pH of 4 with H_2SO_4 at a temperature of 40 ^oC and a constant stirring of 300 rpm.

A potentiodynamic scan with a concentration of 1 mM of SLS was performed as in the iron/molybdenum nanowires, since this was the best concentration that maximized the rate and had less noise on the polarization curve that indicated hydrogen bubbles were being readily removed from the surface. The plot for the potentiodynamic study is shown in the Fig. 5. As shown, there is a shift of the peak from -1 V to a -0.8 V vs SCE compared to Fe-Mo potentiodynamic plote (Fig. 2).

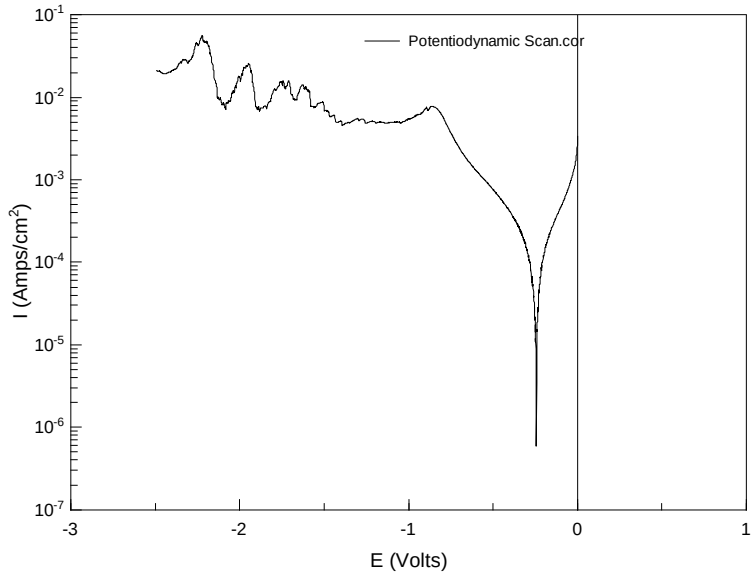


Figure 5. Potentiodynamic plot obtained during the study of Ni-Mo nanowires growth.

For this set of experiments, the nanowires were deposited at pH 4 using the same pulsed potential times of 2 seconds for each step. The selected potentials were -0.6 V to -1.4 V vs SCE to ensure that the deposition takes place after the peak located at -1V. The plot obtained for pH 4 is shown in the Fig. 6, where the intensity of the current density didn't reach significantly positives values during the growth time. The total growth time in all experiments for this nanowires' alloy were 5000 seconds; the necessary time to reach the top.

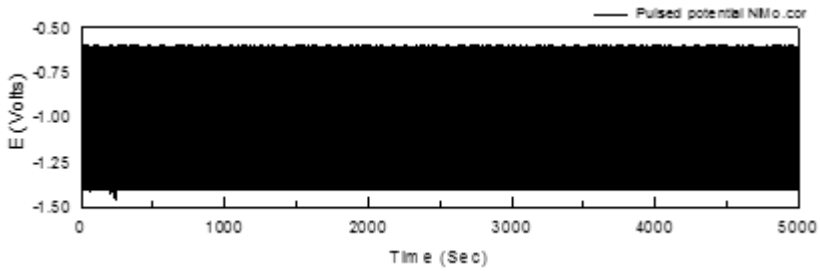


Figure 6. Pulsed potential plot obtained during the growth of Ni-Mo nanowires.

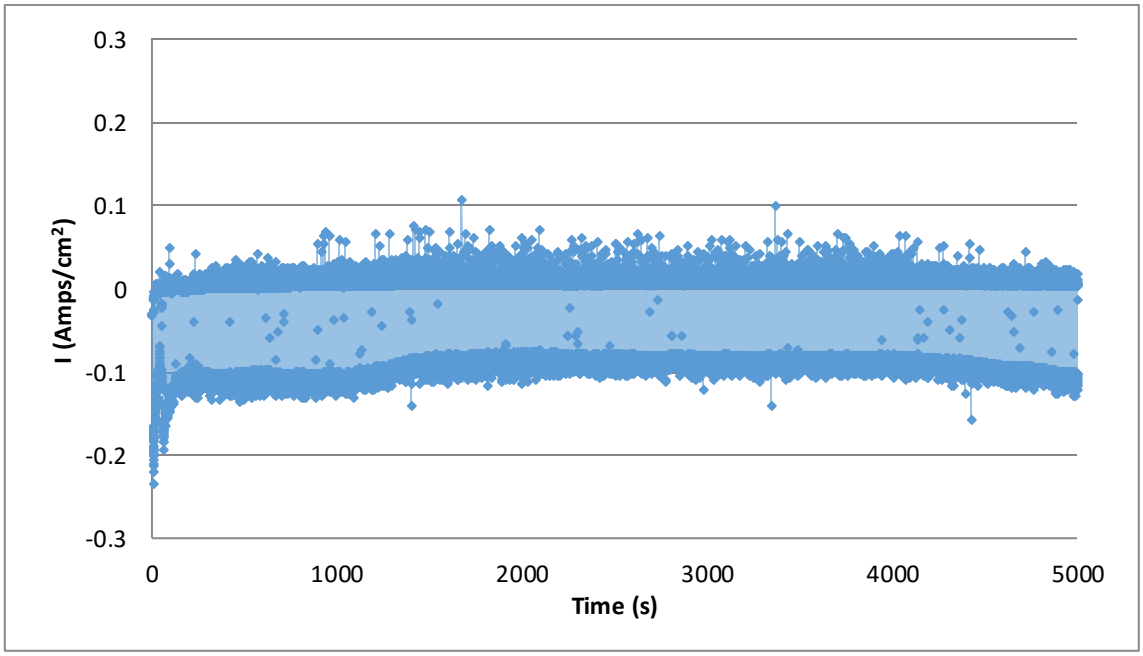


Figure 7. Intensity vs time plot with a stable pulse during time, reaching negligible positive potentials.

Due to a lower catalytic activity this alloy produces a lower concentration of hydrogen which can be efficiently removed from the cathode's surface with the assistance of the surfactant and also with the 2 seconds "off" time relaxation. Therefore, the nanowires were successfully grown.

4.3. Ni-Fe-Mo nanowires

Nickel-molybdenum nanowires were electrodeposited with the same conditions and with the following modification of the electrolyte: 0.1 M nickel sulfate, 0.025 M iron sulfate, 0.01 M sodium molybdate (VI), 0.4 M trisodium citrate, 0.001 M sodium lauryl sulfate, 0.5 M boric acid, 0.002 M saccharine, 1 M boric acid at an adjusted pH of 4. The potentiodynamic study for this ternary alloy was performed and the result is shown in Fig 8. The plot shows two different peaks at values of -0.55 V and -1 V vs SCE.

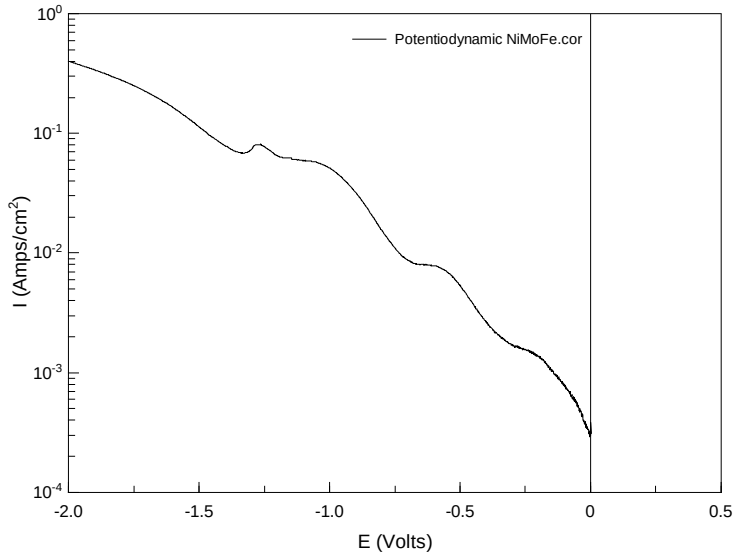


Figure 8. Potentiodynamic study for the Ni-Fe-Mo nanowires alloy. A peak can be interfered at -0.5 V vs SCE.

The experimental parameters were -0.35 V "off" time and -1.15 V "on" time with a cycle of 2 seconds for each condition, as it can be shown in Fig. 9. The total growth time was for all the experiments 5000 seconds; the time needed to reach the top. Also important to note is that the intensity of the current in all experiments didn't reach positive values or negligible values.

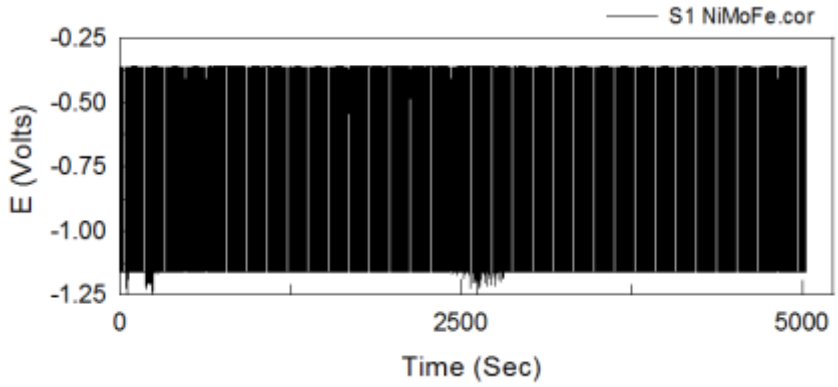


Figure 9. Pulsed potential plot obtained from the growth of Ni-Fe-Mo nanowires alloy.

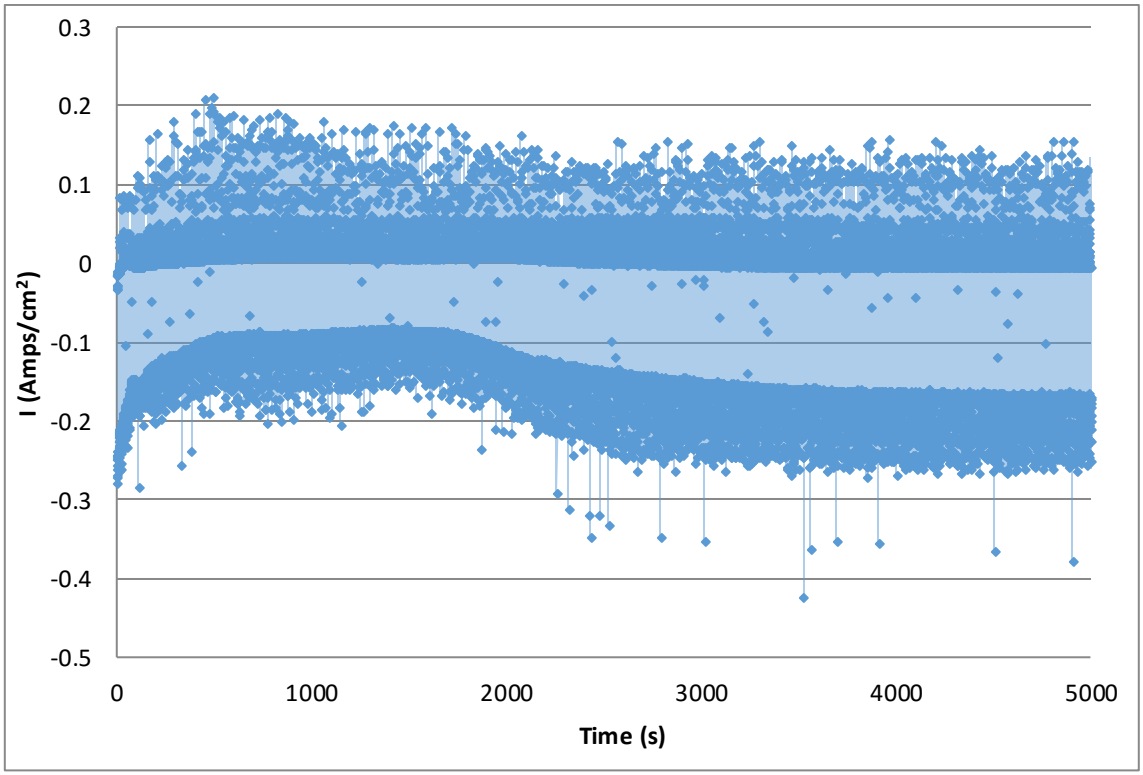


Figure 10. Intensity vs time plot for Ni-Fe-Mo nanowires were it can be interfered that the intensity keeps negative values reaching negligible positive values.

Nanowires were successfully grown with this composition. Nickel has a lower catalytic activity than iron, therefore, it suppresses iron hydrogen catalyst activity enabling the system to grow without the interference of hydrogen.

3.5 Copper displacement OCP study

The open circuit potential (OCP), is the potential of the working electrode relative to the reference electrode when no current is being applied to the cell. A change in the OCP with time, reflects a change in surface conditions. To test the displacement approach, a variation of the OCP should occur as a REDOX reaction involving the metals is occurring. To perform this study a sample containing Ni-Fe-Mo nanowires is dipped for 30 seconds into the copper solution and the OCP vs SCE is measured during the time. The parameters of the solution used for the displacement consist of: 0.15 M copper sulfate, 0.45 M trisodium citrate, 0.01 M sodium sulfate, 0.40 M boric acid at an adjusted pH of 1 using H_2SO_4.

The study of the OCP vs SCE shows a change from low positives values towards a high positives values as the displacement is taking place. Therefore, this study confirms that a reaction without applied current is proceeding. Fig. 11 shows the plot of both the OCP while not and while the reaction is.

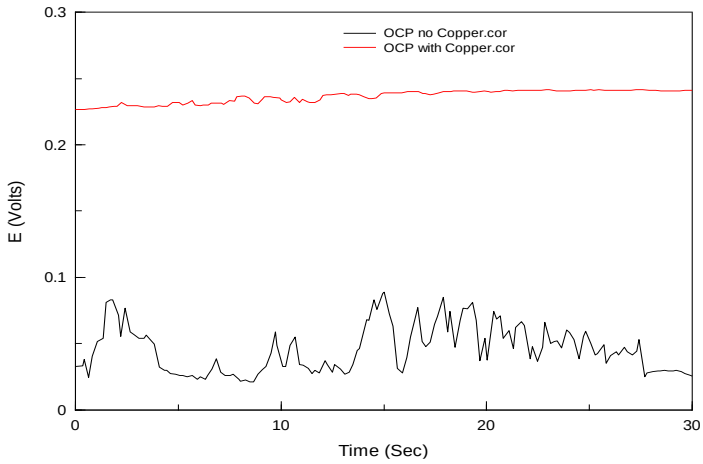


Figure 11. OCP vs SCE difference presented when the system is in a steady state (black) and when displacement reaction takes place (red).

5. Nanowire characterization

5.1. Fe-Mo nanowires

Due to the high catalytic activity of this alloy, the hydrogen present in the system is high enough to block all the pores preventing the deposition of a significant amount of material, therefore none of the experiments were successful. The presence of the surfactant, and longer "off" time times to enable the removal of hydrogen hadn't been efficient enough to enable the deposition.

5.2. Ni-Mo nanowires

Nickel as being part of the iron group it has been reported to enable the codeposition of molybdenum, in the present work for this alloy the characterization techniques used were XRF and SEM imaging. In the following table the XRF results are presented:

Table 1. XRF average composition for Ni-Mo nanowires.

Points	Ni wt%	Mo wt%
1	92	8
2	95	5
3	95	5
4	93	7
5	88	12
Mean	93	7

The polycarbonate membrane has not a defined distribution of the pores, therefore there would be areas in the sample where a major concentration of pores can be found and subsequently the amount of material would be greater. From a selected sample, 5 points are analyzed with a *KevexSpectrace Omicron XRF*, using a collimator with an aperture of 100 microns. The amount of molybdenum deposited in the nanowires is reported to be on average 7 % and the nickel 93 %.

The nanowires are released from the membrane using dichloromethane, and they are rinsed in an ethanol solution.

5.2.1. Ni-Mo-Cu nanowires

Ni-Mo nanowires were dipped in the copper solution for different times to displace as much nickel as possible, the selected times were 0.5, 1, 18 hours. The results obtained are shown in the following table.

Table 2. Average XRF compostion of nanowires after the copper displacement reaction treatment during the studied times.

Time (h)	Ni wt%	Mo wt%	Cu wt%
0	93	7	0
0,5	87	9	4
1	77	14	9
18	89,3	2,6	8

As indicated from Table 2 the amount of nickel that can be displaced reached a steady value after 1 hour dipped in the displacement solution. The variation in the molybdenum concentration can be attributed to two main factors; the 5 points analyzed are not the same in each XRF characterization and also locally the amount of nickel is being decreased by corrosion raising the ratio of molybdenum versus the structure. Finally, at 18 h the sample was degraded, in other words corroded, due to the low pH value (pH= 1) and therefore the results have been affected. Fig. 12 shows the decrease of nickel as the copper is being incorporate to the structure and slight rise on the molybdenum present in the structure.

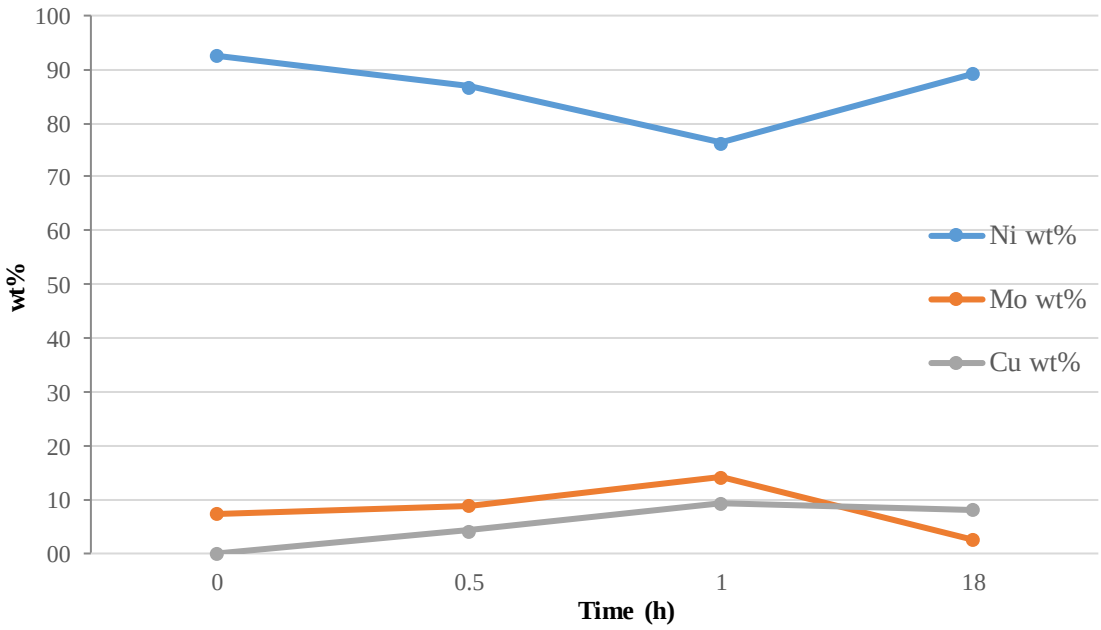


Figure 12. Effect on the nanowires composition vs time after the copper displacement treatment.

5.3. Ni-Mo-Fe nanowires

Since the Ni-Mo nanowires were satisfactory the next aim was to increase the amount of molybdenum present in the structure. Although Fe-Mo nanowires couldn't be deposited, the combination of nickel and iron in the same solution decreased the catalytic activity enough to enable the deposition of the nanowires. The ratio of nickel to iron present in the solution is 4:1, and a higher concentration of nickel is expected to be present in the structure. However, as presented in Table 3, the iron present in the structure is three times higher than the nickel concentration.[13] This phenomenon is called anomalous codeposition and takes place when nickel discharge is suppressed; this suppression is usually found when the pH is high enough to cause hydroxide formation. When the growth of nanowires is taking place there is a local rise of the pH between the surface of the cathode and the solution creating an interface with higher pH; leading to the formation of hydroxide. Therefore, iron is deposited in a higher amount rather than nickel.

Table 3. Average concentration diplayed by XRF of Ni-Fe-Mo-Cu nanowires after the copper displacement treatment.

Points	Ni wt%	Mo wt%	Fe wt%
1	16,1	29,3	54,6
2	17,0	25,9	57,1
3	18,4	24,6	56,9
4	17,5	23,2	59,2
5	19,0	24,9	56,2
Mean	17,6	25,6	56,8

Fig. 13 shows the images obtained using a scanning electron microscope (SEM) show robust continuous and non-porous nanowires. It is also important to notice that nanowires stick together due to the magnetic effect exercised by the iron; sonication has been proved to be a good way to spread them apart but at the same time long times under sonication leads to the breakage of the nanowires. The total length of the unbroken nanowires was around 6 microns as it was expected.

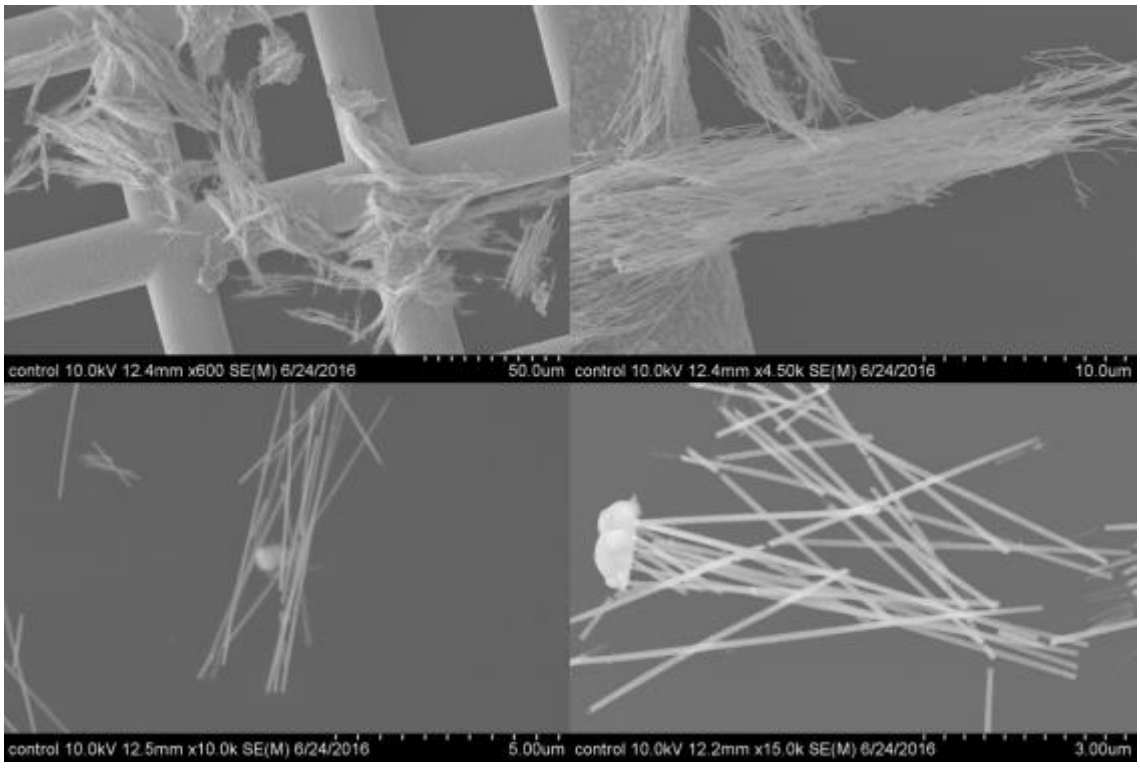


Figure 13. SEM images from lower mangnitude to higher of Ni-Fe-Mo nanowires.

Fig. 14 shows the images acquired using transmission electron microscope (TEM).

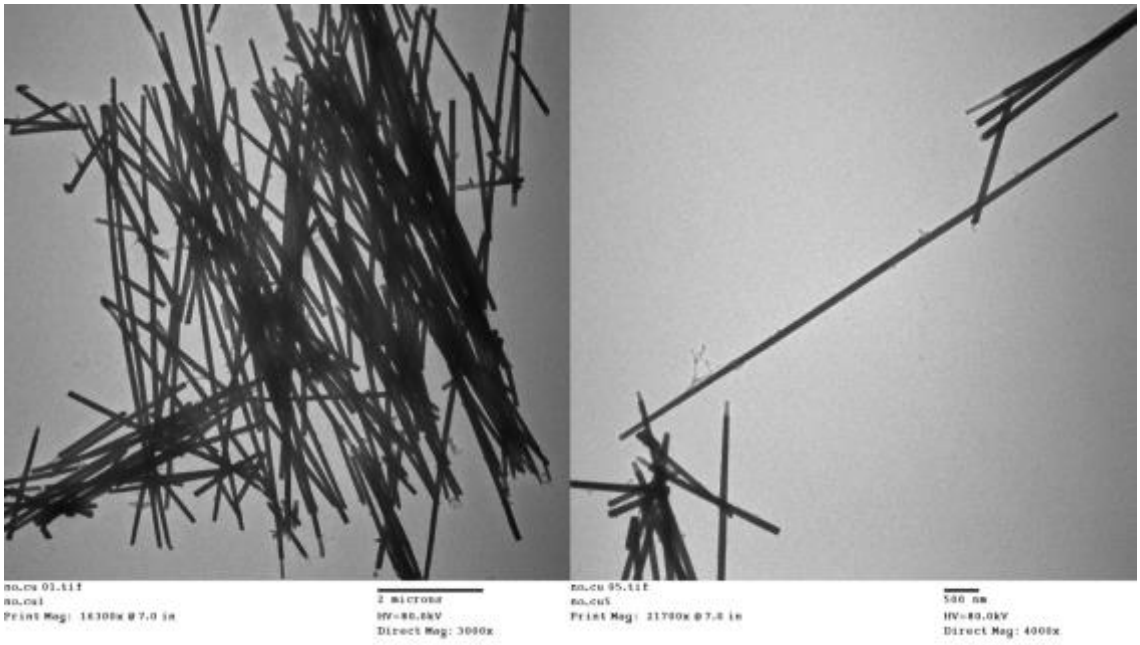


Figure 14. TEM images of Ni-Fe-Mo nanowires.

5.3.1. Ni-Fe-Mo-Cu nanowires

Once the Ni-Fe-Mo nanowires were grown inside the pores of the membrane, the whole sample was dipped in the displacement solution. As it has been discussed in the copper displacement approach paragraph, iron is expected to be displaced faster than nickel. The selected times for this set of experiments were 30, 45, 60, 120 seconds. In the Table 4 the results for each time are being displayed. It is also important to highlight that at bare eye it can be seen a change on the surface of the membrane from dark grey to the typical copper brown orange.

Table 4. Average concentration of Ni-Fe-Mo-Cu nanowires after the displacement reaction with copper.

Time (s)	Ni wt%	Mo wt%	Fe wt%	Cu wt%
0	17,6	25,6	56,8	0,0
30	12,3	22,8	32,7	32,2
45	6,6	18,0	20,3	55,1
60	7,6	19,4	20,8	52,2
120	2,6	15,3	13,5	68,6

Fig. 15 shows the evolution of the displacement in function of time, it can be seen that both nickel and iron are being displaced and their concentration decrease meanwhile the concentration of copper increases. The loss of molybdenum during the process is around a 5% until 60 seconds. For 120 seconds the loss of molybdenum is a

10% which suggest that the optimum time to perform the displacement and obtain the most higher concentration of copper is 60s.

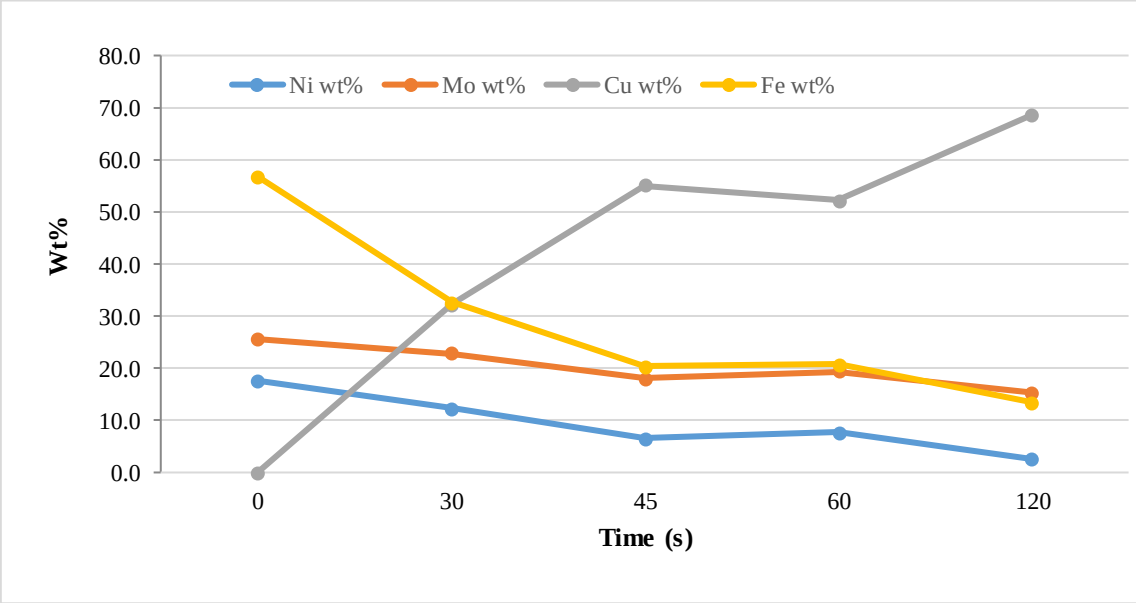


Figure 15. Evolution of the average composition during the time after the copper displacement has been performed.

Fig. 16 present the TEM images for Ni-Mo-Fe-Cu nanowires after being dipped in the solution and released from the membrane. As can be seen there is a change in the color of the structure were the copper has been placed. The top of the nanowire is brighter than its body suggesting that the copper is being introduced to the structure from top to bottom in a gradient, finding the higher concentration of copper at the top.

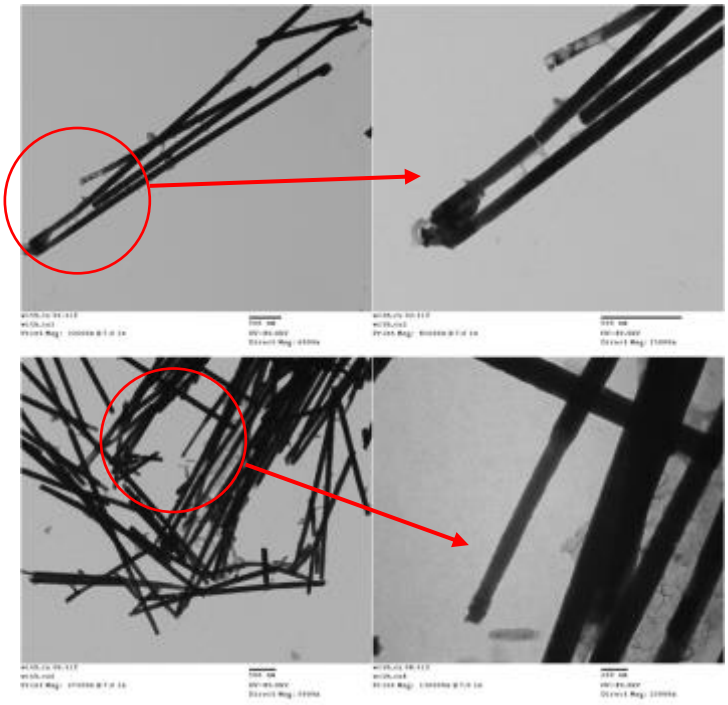


Figure 16. TEM images of the Ni-Fe-Mo-Cu nanowires, left images correspond to low magnification and right ones a high magnification. Copper has a brighter color in contrast to the body of the nanowire which is dark.

A Ni-Fe-Mo-Cu sample which had been dipped for 30s was studied under a HRTEM and a diffraction study was carried out. The results are shown in Fig. 17 where it can be seen that the top of the nanowire has a clearly different diffraction pattern than the rest of the body confirming, with the X-ray results, that copper has been successfully added to the nanowire structure.

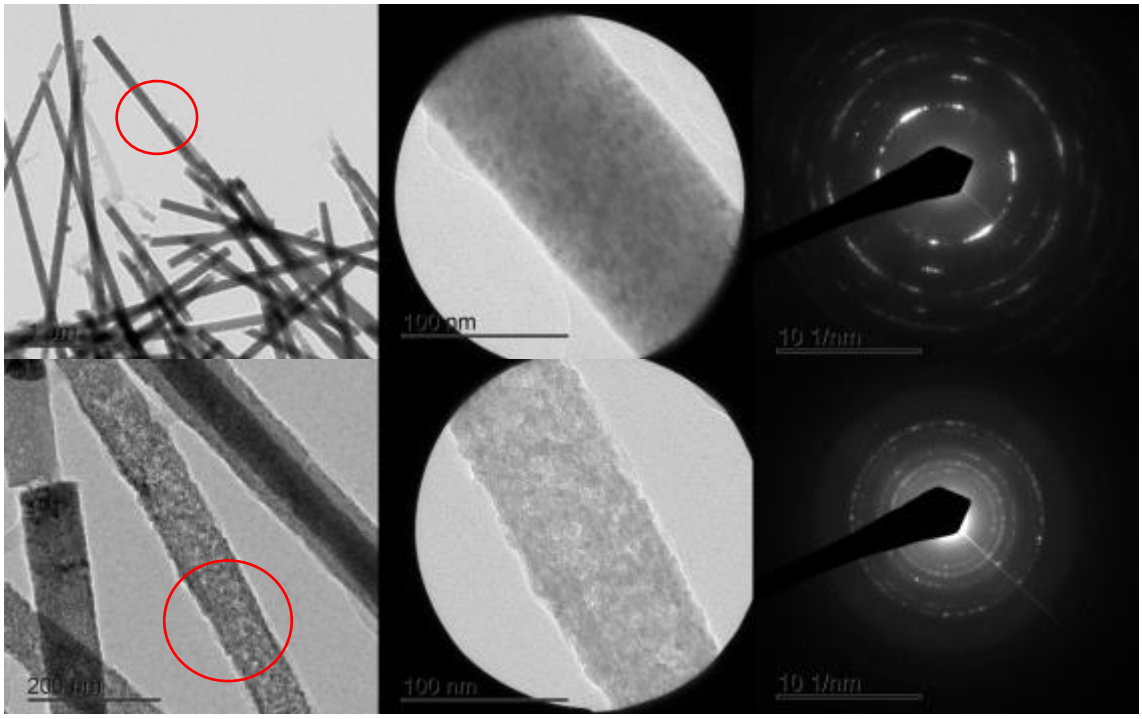


Figure 17. Images and diffraction patterns obtained with HRTEM. Top image shows the diffraction pattern from the middle body of the nanowire. Bottompattern shows the diffraction of the top section of the nanowire where the Cu displacement reactions occurs.

6. Conclusions

In this work four different nanowire alloys have been deposited successfully, Ni-Mo, Ni-Mo-Cu, Ni-Mo-Fe and Ni-Mo-Fe-Cu. Due to the high catalytic activity of Fe-Mo nanowires those have could not be deposited even having taken measures to reduce the impact of the hydrogen formation. The nanowires obtained using a pulse potential growth method have presented a continuous, non-porous and robust structure. The length expected was 6 microns and it has been satisfactorily achieved. A concentration up to 25% of molybdenum have been obtained combining nickel and iron as inducing metals, and the loss of molybdenum after the treatment of copper is a 5% in the Ni-Fe-Mo-Cu alloy. The higher concentration of copper introduced in the structure it is found on the top as it is where the displacement occurs in first place and in a gradient the concentration is lowered as it gets deeper into the structure.

7. Acknowledgment

This work has been supervised by Dr. Podlaha-Murphy and has been developed in her research group. I would like to thank all the members of the group Dr. Avinash Kola, Xiaohua Geng, Deyang Li and Yujia Zhang for their support and help when I

needed and also I am especially thankful with Dr. Podlaha-Murphy for her support, guidance and help.

8. Bibliography

Hydrogen catalysis

1. E. Navarro-Flores, Z. Chong and S. Omanovic, *Characteritzation of Ni, NiMo, NiW and NiFe electroactive coatings as electrocatalysts for hydrogen evolution in an acidic medium*, *J. Mol. Catal. A: Chem.*, 226 (2005).
2. Gonzalez-Buch C., Herraiz-Cardona I., Ortega E., Garcia-Anton J., Perez-Herranz V., *Development of Ni-Mo, Ni-W and Ni-Co Macroporous Materials for Hydrogen Evolution Reaction*, Chem. Eng. Trans. 32, (2013).
3. Fan, C.; Piron, D.L.; Sleb, A.; Paradis, P, (1994) *"Study of electrodeposited nickel-molybdenum, nickel-tungsten, cobalt-molybdenum, and cobalt-tungsten as hydrogen electrodes in alkaline water electrolysis," Journal of the Electrochemical Society*, vol. **141**, 382-387.

Electrodeposition, codeposition and mechanisms

4. N. Tsyntsaru, H. Cesiulis, M. Donten, J. Sorte, E. Pellicer, and E. J. Podlaha-Murphy**,** *"Modern Trends in Tungsten Alloys Electrodeposition with Iron Group Metals***,"** *Surface Engineering and Applied Electrochemistry,* vol. **48** (6) 491–520 (2012).)
5. A. Brenner, *Electrodeposition of Alloys: Principles and Practice.* Academic Press, New York, 1963.
6. O. Younes and E. Gileadi, *Electroplating Ni/W alloys of I. Ammoniacal citrate baths*, J. Electrochem. Soc., vol. **149**, no. 2, pp. C100-C111, Feb. 2002.
7. O. Younes-Metzler, L. Zhu, and E. Gileadi, *The anomalous codeposition of tungsten in the presence of nickel*, Electrochim. Acta, vol. **48**, no. 18, pp. 2551-2562, Aug. 2003.
8. N. Eliaza and and E. Gileadi, *The Mechanism of Induced Codeposition of Ni-W Alloys,* ECS Trans., vol. 2, no. 6, pp. 337-349, 2007.
9. E. J. Podlaha and D. Landolt, *Induced codeposition. I. An experimental investigation of Ni-Mo alloys,* J. Electrochem. Soc., vol. **143**, no. 3, Mar. 1996.
10. E. J. Podlaha and D. Landolt, *Induced codeposition. II. A mathematical model describing the electrodeposition of Ni-Mo alloys,* J. Electrochem. Soc., vol. 143, no. 3, Mar. 1996.
11. E. J. Podlaha and D. Landolt, *Induced codeposition. III. Molybdenum alloys with nickel, cobalt, and iron,* J. Electrochem. Soc., vol. **144**, no. 5, pp. 1672-1680, May 1997.
12. Ved', M. V., Sakhnenko, N. D., Karakurchi, A. V., & Zyubanova, S. I. (2014). Electrodeposition of iron-molybdenum coatings from citrate electrolyte. *Russian Journal of Applied Chemistry*, *87*(3), 276–282.
13. Force, A., Sothern, R. D., Cooke, S. L., Goodwyn, J. R., Cleaves, H. E., Stachurski, Z., … Hoare, J. P. (n.d.). J. Phys. Chem., 58, 951 (1954). 2., *112*(8), 6–10.

14. Kola, A. R., & Podlaha, E. J. (2011). Electrodeposition of Ni-W , Ag-W and Ag-Ni-W Alloys from Citrate-Thiourea Electrolytes, *1409*(1903), 2013.
15. Izaki, M. (2011). Modern Electroplating. *Modern Electroplating*, 309–326.

General aspects of metals

16. Copper properties and uses. Introduction. (n.d.). Retrieved April 8, 2016, from http://resources.schoolscience.co.uk/CDA/14-16/chemistry/copch0pg5.html
17. Applications of Molybdenum Metal and Its Alloys - IMOA. (n.d.). Retrieved April 10, 2016, from http://www.imoa.info/download_files/molybdenum/Applications_Mo_Metal.pdf